Surface Modified Nanocellulose Fibers Yield Conducting Polymer-Based Flexible Supercapacitors with Enhanced Capacitances

Zhaohui Wang,*,† Daniel O. Carlsson,‡ Petter Tammela,‡ Kai Hua,‡ Peng Zhang,‡ Leif Nyholm,*,† and Maria Strømme*,‡

†Department of Chemistry-The Ångström Laboratory, Uppsala University, Box 538, SE-751 21 Uppsala, Sweden and ‡Nanotechnology and Functional Materials, Department of Engineering Sciences, The Ångström Laboratory, Uppsala University, Box 534, SE-751 21 Uppsala, Sweden

ABSTRACT We demonstrate that surface modified nanocellulose fibers (NCFs) can be used as substrates to synthesize supercapacitor electrodes with the highest full electrode-normalized gravimetric (127 F g^{-1}) and volumetric (122 F cm^{-3}) capacitances at high current densities (300 mA cm^{-2} ≈ 33 A g^{-1}) until date reported for conducting polymer-based electrodes with active mass loadings as high as 9 mg cm^{-2}. By introducing quaternary amine groups on the surface of NCFs prior to polypyrrole (PPy) polymerization, the macropore volume of the formed PPy-NCF composites can be minimized while maintaining the volume of the micro- and mesopores at the same level as when unmodified or carboxylate groups functionalized NCFs are employed as polymerization substrates. Symmetric, aqueous electrolyte-based, devices comprising these porosity-optimized electrodes exhibit device-specific volumetric energy and power densities of 3.1 mWh cm^{-3} and 3 W cm^{-3} respectively; which are among the highest values reported for conducting polymer electrodes in aqueous electrolytes. The functionality of the devices is verified by powering a red light-emitting diode with the device in different mechanically challenging states.

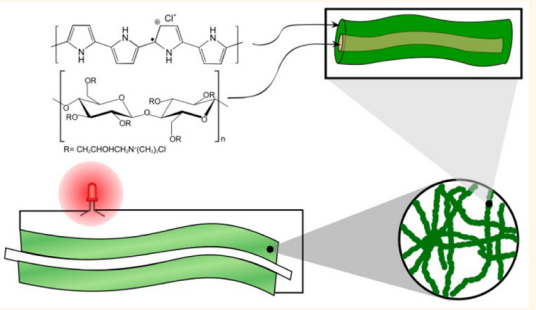

KEYWORDS: energy storage devices · conducting polymers · modified nanocellulose · porosity optimization · capacitance

Supercapacitors have received extensive attention owing to their high power densities and excellent cycle life.[1] With an increasing demand for portable and wearable energy storage devices, recent research has focused primarily on improving the energy densities and capacitances per unit volume of the supercapacitors.[2−4] Currently, great performances have been realized by carbon materials with active mass-normalized volumetric capacitances in the range of 100−500 F cm^{-3},[3,5−9] and two-dimensional carbides with even higher capacitances (~200−900 F cm^{-3}).[2,4,10−12] Electroactive conducting polymers (ECPs), such as polypyrrole (PPy) and polyaniline (PANI), have also developed into a promising class of materials for supercapacitor electrodes due to their inherent high capacities, flexibility, and versatility, as well as their light weight and inexpensiveness.[13−15] Even though extensive progress in the development of ECP-based electrodes has been made, the latter electrodes are not yet able to compete with carbon and carbides electrodes regarding volumetric capacitance. The quest for sustainable and inexpensive ECP-based electrodes with high volumetric capacitance therefore still constitutes a challenge.

Conventional supercapacitors are often still too heavy, thick, rigid, and bulky to fully meet the practical requirements for portable devices due to the presence of inactive components, such as heavy metal substrates, binders, and conductive additives.[16] Hence, there is an urgent need to develop lightweight and flexible ECP-based supercapacitors with high volumetric capacitances. Such progress requires the development of methods for fabrication of freestanding and flexible electrodes containing minimum

* Address correspondence to zhaohui.wang@kemi.uu.se, leif.nyholm@kemi.uu.se, maria.stromme@angstrom.uu.se.

Received for review May 11, 2015 and accepted June 17, 2015.

Published online June 17, 2015
10.1021/acsnano.5b02846

amount of inactive materials. Recently, several substrates have been tested for flexible ECP-based supercapacitors electrodes, including plastics, textiles, graphene paper and cellulose papers.[14−23] Among these flexible substrates, cellulose, which is the most abundant biopolymer on earth and the major component in paper, is particularly promising because of its environmental friendliness, high mechanical performance, flexibility, low-cost, versatility, and tailorable surface functionalities.[14,24,25]

Significant efforts have been made to design paper-based flexible ECP composites supercapacitor electrodes with improved capacitances. Poly(ethylenedioxythiphene) (PEDOT) coated cellulose electrodes have, for example, been shown to exhibit a specific volumetric capacitance of 145 F cm^{-3} at 0.4 mA cm^{-2} when normalized with respect to the active material volume, but only 35 F cm^{-3} when normalized with respect to the volume of the entire electrode.[26] Flexible PANI/Au/paper has been found to exhibit a volumetric capacitance of 800 F cm^{-3} at 1 mA cm^{-2} based on the volume of the active PANI layer.[22] For practical applications, the volumetric capacitances, based on the full electrode volume, as well as the rate capability of such electrodes need to be significantly improved. Recently, we demonstrated that compact PPy-nanocellulose fiber (PPy-NCFs) electrodes can be compressed to yield volumetric capacitances exceeding 236 F cm^{-3} (or 192 F g^{-1}) based on the full electrode volume at 1 mA cm^{-2}.[27] Such electrodes are, however, inflexible and have full electrode based gravimetric capacitances of only 75 F cm^{-3} (or 61 F g^{-1}) at 200 mA cm^{-2}. More recently, we have shown that NCFs containing flexible, yet compact, PPy-covered graphene oxide electrodes can yield a specific electrode capacitance of 198 F cm^{-3} (or 244 F g^{-1}) at 200 mA g^{-1},[15] however, with a modest rate capacity of 86 F cm^{-3} (or 107 F g^{-1}) at 10 A g^{-1}. Based on these current scientific accomplishments it remains a considerable challenge to simultaneously achieve both high gravimetric and volumetric capacitances while retaining excellent rate capability for flexible ECP-based electrodes.

Here, we use unmodified (u-NCFs) or modified NCFs to obtain flexible PPy-NCF electrodes with high gravimetric and volumetric capacitances. Two well-known NCF modification processes were employed to introduce carboxylate or quaternary amine groups, resulting in fibers with anionic (a-NCFs) or cationic (c-NCFs) surface charges (at neutral pH and low ionic strength), respectively (See Figure 1). These fibers, and films thereof, have been prepared and characterized according to our earlier work.[28] We show that when c-NCFs are used as the substrate for PPy electrode fabrication, the highest full electrode normalized gravimetric (127 F g^{-1}) and volumetric (122 F cm^{-3}) capacitances until date reported at high current densities (300 mA $cm^{-2} \approx$ 33 A g^{-1}) for an ECP-based electrode

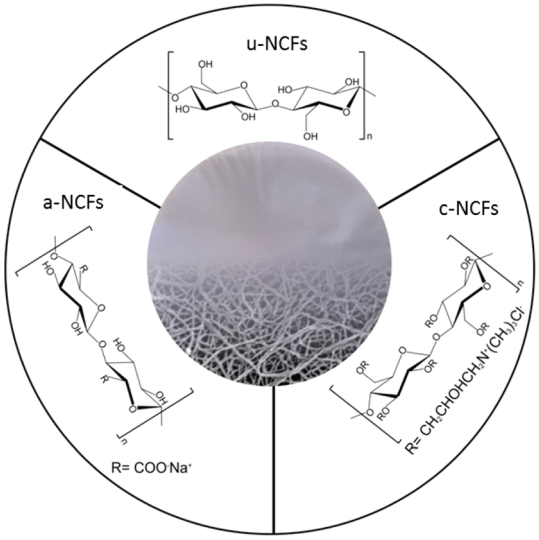

Figure 1. Photograph of NCFs paper and molecular structure of NCFs.

are obtained. We further show that the composites easily can be integrated into miniaturized flexible devices which can power a red light-emitting diode with the device in different mechanically challenged states. Symmetric devices comprising these electrodes yield device-specific volumetric energy and power densities of 3.1 mWh cm^{-3} and 3 W cm^{-3}, respectively, which are among the highest values for conducting polymers electrode in aqueous electrolytes.

RESULTS AND DISCUSSION

Zeta-potential measurements performed at pH 7 on all three types of cellulose fibers used in the present study gave values of −12, −41, and +31 mV for u-NCFs, a-NCFs, and c-NCFs, respectively,[28] thus confirming successful surface modification of the a-NCFs and c-NCFs fibers with carboxyl groups or quaternary ammonium groups, respectively. This was also corroborated by Fourier transform infrared spectroscopy measurements (Figure S1). After polymerization of pyrrole in the presence of u-NCFs, c-NCFs, and a-NCFs (Figure 1), composites with the appearance of black papers are formed (inset in Figure 2a). The composites comprise numerous intertwined fibers with a porous structure (Figure 2a−c), in good agreement with our previous results for other types of PPy-NCFs composites.[27,29] More specifically, all three samples exhibit nearly identical PPy weight ratios (Figure S2) and a PPy mass loading of ∼9 mg cm^{-2} (see Methods). The type of modification of the cellulose nanofibers was found to have significant impact on the mechanical properties of the composites (see Figure S3). The PPy@c-NCFs paper exhibited the highest tensile strength and Young's modulus of the composites; about 14.3 MPa and 1.3 GPa, respectively, compared to 6.6 MPa and 0.73 GPa for PPy@u-NCFs, and 2.3 MPa and 0.39 GPa for PPy@a-NCFs. The PPy@c-NCFs also demonstrated

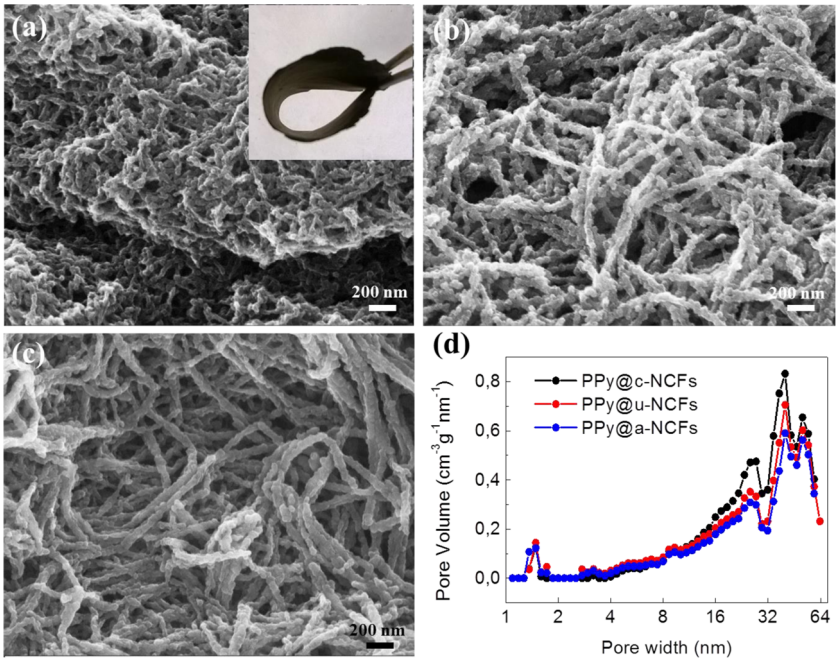

Figure 2. SEM images for PPy@c-NCFs (a), PPy@u-NCFs (b), PPy@a-NCFs (c), and their pore size distributions (d).

excellent mechanical flexibility and could be bent several times (see Figure 2a) without crack-formation in the material. The PPy@u-NCFs and PPy@a-NCFs composites were found to be less flexible and behaved as rather rigid, freestanding paper sheets.

The micrographs of the three composite types under study (Figure 2a−c) revealed some differences on the micro and nanoscale. Although all three sample types displayed fibrous and porous structures, PPy@u-NCFs and PPy@a-NCFs appeared to have a loosely interconnected fibrous structure, while PPy@c-NCFs appeared to be more densely packed when compared with the other two composites.

The difference in morphology observed *via* scanning electron microscopy (SEM), with PPy@c-NCFs appearing to be significantly denser than the other two samples, was confirmed through porosity determinations. The porosity of the samples was found to be 38%, 56%, and 62% for PPy@c-NCFs, PPy@u-NCFs, and PPy@a-NCFs, respectively, whereas the corresponding specific surface areas (SSAs) were 69, 86, and 83 $m^2 g^{-1}$, respectively, as obtained from a BET analysis of N_2 adsorption isotherms (Figure S4). Thus, it can be concluded that different degrees of PPy-NCF aggregation can be achieved through modification of the NCFs acting as substrates for PPy polymerization. Consequently, the bulk density of the composite was 0.96 g cm^{-3} for the PPy@c-NCFs, compared with 0.70 g cm^{-3} for PPy@u-NCFs and 0.60 g cm^{-3} for PPy@a-NCFs. Interestingly, the N_2 sorption isotherms are very similar (and of type IV) for all three sample types under study, indicating the presence of both micro- and mesopores. The latter is further supported by the pore size distribution curves obtained from density functional theory evaluation of the N_2 sorption data (Figure 2d). Such structures have previously been shown to be beneficial for efficient and fast charge storage in the PPy layer of PPy-NCFs composites.[27]

The fact that the micro- and mesopore structures of the three composite types are almost identical (Figure 2d) while the total porosity of PPy@c-NCFs is significantly lower than that for the other two composites, shows that the employment of the c-NCFs substrate yields a porosity-optimized composite in which only the macropore volume is reduced as compared to when other types of NCFs substrates are used. Reducing the macropore volume while maintaining the volume of micro- and mesopores is expected to be beneficial for the electrochemical properties of the composite since this reduces the redundant electrolyte weight while still allowing for good access of the electrolyte to a large portion of the electroactive material.[27] This is, as far as we know, the first time such a porosity optimization has been achieved for ECP-based composites merely by chemical modification of the polymerization substrate without using external pressure or different cellulose drying steps.

The present results clearly show that the use of the c-NCFs give rise to a material with a higher density and with a lower surface area than the corresponding materials obtained with the a-NCFs and u-NCFs, respectively. The absence of a significant difference between the densities and surface areas for the PPy@u-NCFs and PPy@a-NCFs composites can likely be explained by the fact that the carboxylic acid groups on the a-NCF fibers should have been protonated (and hence uncharged) under the experimental conditions employed during the PPy polymerization

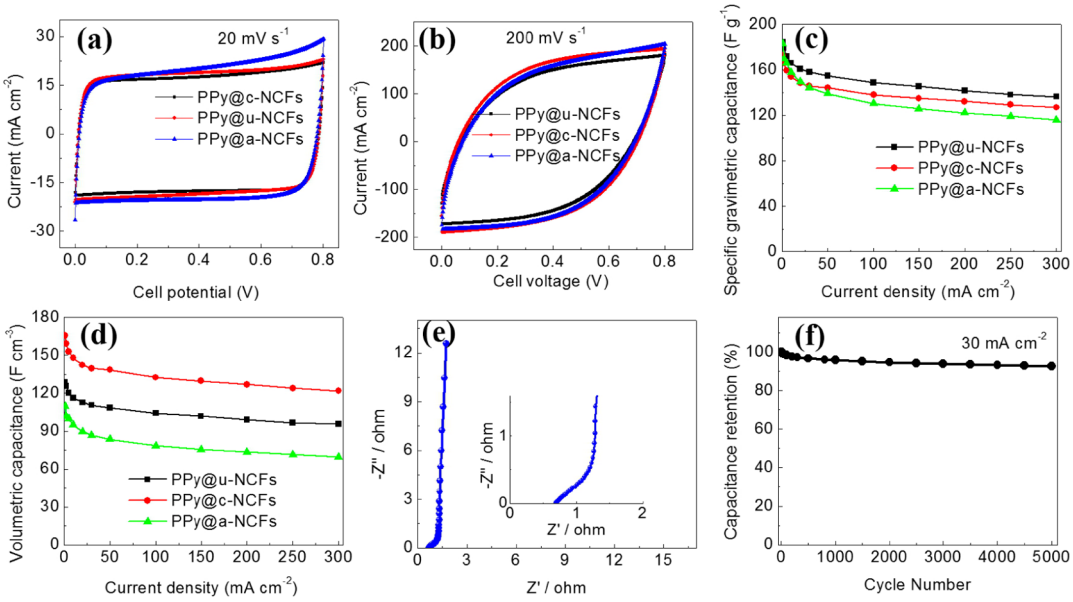

Figure 3. Electrochemical characterization of composite electrodes in 2.0 M NaCl recorded with symmetric supercapacitor devices. CV curves for scan rates of (a) 20 and (b) 200 mV s^{-1}. (c) Gravimetric and (d) volumetric capacitances for different charging/discharging current densities (see Figure S5). (e) Nyquist plot and (f) cycling performance in terms of capacitance retention at 30 mA cm^{-2} for a PPy@c-NCFs based device (the capacitance from the first cycle is set to 100%).

(*i.e.*, pH ∼ 0.5). Similarly it would have been expected that the high ionic strength (*i.e.*, $[Cl^-]$ = 0.6 M) would lead to screening of the cationic charges of the c-NCF fibers, and from this perspective similar composite structures would be anticipated irrespective of the NCF used. Previous findings with NCF films, that is, pure cellulose films, demonstrated that the BET surface area for u-NCFs (102 m^2 g^{-1}) was significantly higher than that for a-NCFs (77 m^2 g^{-1}) and c-NCFs (70 m^2 g^{-1}).[28] In that case, the experiments were carried out in deionized water; that is, the carboxylic acid groups were deprotonated and the quaternary ammonium groups were not screened, indicating that the presence of charged groups on the cellulose fibers gives rise to more compact materials with smaller surface areas. In the current work, it thus seems possible that the surface charges of c-NCF are not completely screened during composite synthesis, but other effects of the cellulose modification cannot be ruled out. While it is known that the drying conditions and the type and amount of NCFs affect the structural properties of PPy-NCFs composites,[30,31] further studies are clearly needed to understand the effect of the cellulose modification on the structure of the obtained composite.

To investigate the charge storage properties of the different PPy-NCFs composites, symmetric supercapacitor cells were assembled with approximately the same electrode masses. Figure 3 presents electrochemical characterization data for these cells obtained in a 2.0 M NaCl electrolyte. The cyclic voltammetry (CV) curves (Figure 3a and b) were found to have a nearly symmetrical, rectangular shape, suggesting an almost ideal pseudocapacitive response. Note that the NCFs did not contribute to the measured electrochemical response (see Figure S6). Figure 3c shows a plot of the specific gravimetric electrode capacitance, C_g (obtained from galvanostatic charge/discharge curves, Figure S5), for all studied device types as a function of the current density. As seen from this figure panel, all three composite types exhibited practically the same gravimetric capacitances at a current density of 1 mA cm^{-2}; that is, ∼180 F g^{-1} composite corresponding to ∼260 F g^{-1} PPy. Also at 300 mA cm^{-2}, the C_g values of the electrodes of the different devices were rather similar to the highest being 136 F g^{-1} (PPy@u-NCFs) and the lowest 116 F g^{-1} (PPy@a-NCFs). Hence, all three samples showed good rate capabilities.

The volumetric capacitances, C_v, of the composites under study were, on the other hand, found to differ substantially as is seen in Figure 3d. The composite with the highest bulk density, PPy@c-NCFs, exhibited the highest C_v value: 173 F cm^{-3} at a current density of 1 mA cm^{-2} and 122 F cm^{-3} at 300 mA cm^{-2} (or 33 A g^{-1}). These values are to the best of our knowledge higher than all values previously reported for ECP-based electrodes particularly as the previous studies were carried out at significantly lower current densities (see Table 1). Moreover, while the mass (or volume) of the entire electrode was used in the present calculations only the mass (or volume) of the active material was taken into account in some reports (thus neglecting the mass (or volume) of the substrate). With the latter approach, C_g and C_v values of 181 F g^{-1} and 174 F cm^{-3} are instead obtained for PPy@c-NCFs at a current density of 300 mA cm^{-2} (or 33 A g^{-1});

TABLE 1. Electrochemical Performance in Terms of the Gravimetric, C_g, and Volumetric, C_v, Capacitances of the Flexible Polymer-Based Electrodes

materials	C_g (F g^{-1})	C_v (F cm^{-3})	ref
compressed APP	82[b] (200 mA/cm^2)	84[b] (200 mA/cm^2)	27
CCF-PPy@GO	107[a] (10 A/g)	86[a] (10 A/g)	15
PPy@GO	90[a] (10 A/g)	112[a] (10 A/g)	15
3D PPy	185[b] (2 mA/cm^2)	72[b] (2 mA/cm^2)	29
PANI-NF	210[a] (0.3 A/g)	160[a] (0.3 A/g)	32
rGO/PANI	233[b] (2 mV/s)	135[b] (2 mV/s)	33
PPy paper	∼150[a] (20 mA/cm^2)	11[b] (1 mA/cm^2)	19
PEDOT/paper	115[a] or 20[b] (0.4 mA/cm^2)	145[a] or 35[b] (0.4 mA/cm^2)	26
PPy@c-NCFs	**181[a] or 127[b] (33 A/g or 300 mA/cm^2)**	**174[a] or 122[b] (33 A/g or 300 mA/cm^2)**	**our work**

[a] Normalized with respect to active mass or volume. [b] Normalized with respect to full electrode mass or volume (including substrate). The literature data represent the highest values given in the references.

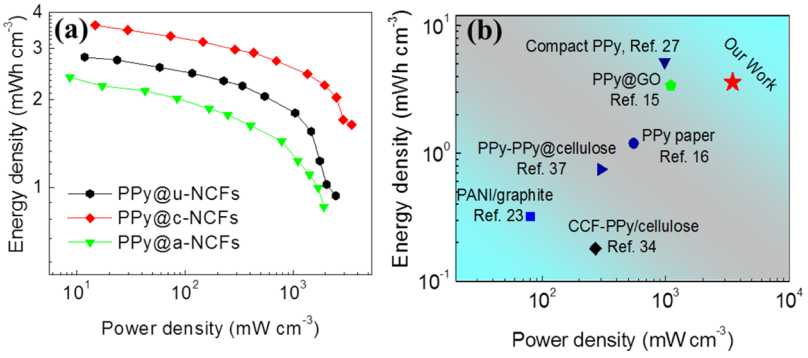

Figure 4. (a) Ragone plots for symmetric supercapacitor devices containing the composite electrodes under study (and a 2 M NaCl electrolyte) upon charging the devices to 0.8 V. (b) Comparison of the Ragone plots of PPy@c-NCFs-based device with those of other conducting polymer based systems. The literature values represent the highest values given in the references.

see Table 1 and Figure S7. The device-specific volumetric capacitance can be obtained by multiplying the volumetric capacitance of two electrodes by the volumetric fraction of the two electrodes in the device (including two electrodes, two current collectors and the separator). Consequently, the PPy@c-NCFs electrode-based supercapacitor exhibits a volumetric capacitance of 149 F cm^{-3} at a current density of 1 mA cm^{-2} and 105 F cm^{-3} at 300 mA cm^{-2} when normalized with respect to whole device.

One of the most important advantages with the present composites is that high mass loadings can be used without loss of the electrochemical properties. Since the active mass per foot print area of the composite electrodes is about nine times higher (∼9 mg cm^{-2}) than the typical active mass loading (1 mg cm^{-2}) used in contemporary supercapacitor electrodes, areal capacitances as high as 1.6 F cm^{-2} at 300 mA cm^{-2} can readily be obtained. The latter value is significantly higher than those previously reported in the literature.[19,34,35] Hence, it is immediately clear that the present composites allow the electrodes to be up-scaled to provide higher energy storage capacities without significant loss of power density. This is a very important point since it is well-known that high gravimetric power densities can be obtained with electrodes containing very small amounts of active material although such electrodes are of little use in practical devices.

Since the PPy@c-NCFs composite exhibited the highest volumetric capacitance as well as the highest energy and power densities (as will be presented below, see Figure 4a) of the samples studied here, the PPy@c-NCFs composite was further studied with electrochemical impedance spectroscopy (EIS). As is seen from the Nyquist plot in Figure 3e, the high-frequency resistance was found to be approximately 0.7 Ω. The absence of a semicircle at frequencies higher than that of the onset of the diffusion limited response (45° sloping line in the Nyquist plot) can be explained by the fact that the charge and discharge rates of the present type of PPy composites has been found to be limited merely by the RC time constant of the cell (which means that the electron transfer rates are too high to be rate determining).[36] At the lowest frequencies, a nearly vertical line is hence observed, indicating an almost ideal capacitive response, in good agreement with previous findings for similar composites.[15,29,37]

Since the cycling stability is a very important issue for supercapacitors, the stability of the symmetric supercapacitor was evaluated in a long-term charge/discharge

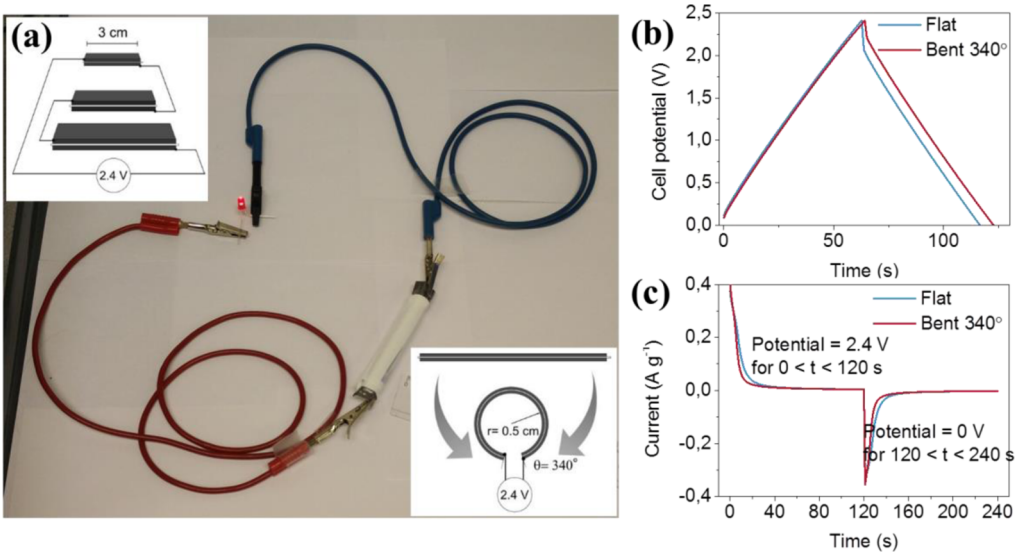

Figure 5. (a) Photo of a red LED powered by three flexible PPy@c-NCFs-based supercapacitors coupled in series for a bending angle of ~340°. (b) Charge/discharge profiles for the in-series supercapacitors under flat and bending conditions for an applied current of ±20 mA as well as (c) the corresponding current responses due to potential steps to 2.4 and 0 V, respectively.

cycling test at 30 mA cm^{-2}; see Figure 3f. The PPy@c-NCFs based symmetric supercapacitor showed excellent cycling stability as 93% of the initial capacitance was maintained after 5000 cycles.

The volumetric energy and power densities normalized with respect to the full electrode weight or volume were also calculated based on the results of the chronopotentiometric experiments in Figure S5 (as is described in the experimental section). A gravimetric energy density of around 4.0 Wh kg^{-1} and a gravimetric power density of 3.5 kW kg^{-1} were obtained after normalization with respect to the weight of both electrodes (see Figure S8). These values are comparable to, or even higher than, those previously presented for PPy-based paper electrodes (*i.e.*, (CCFs-PPy@cellulose,[34] 0.61 Wh kg^{-1} and 0.95 kW kg^{-1}), (cellulose-PPy@GO,[15] 5.1 Wh kg^{-1} and 1.5 kW kg^{-1}), (PPy nanofiber-PPy@cellulose,[37] 3 Wh kg^{-1} and 1.2 kW kg^{-1})). When translated into volumetric energy and power densities, the performance of the present electrodes is, however, more notable. As shown in Figure 4a, the compact structure of the PPy@c-NCFs composite gave rise to significantly higher volumetric energy and power density than those containing a-NCFs or u-NCFs. The volumetric energy density for the PPy@c-NCFs composite electrodes was thus 3.6 mWh cm^{-3}, which is comparable to that for many commercial carbon/carbon capacitors (~5 mWh cm^{-3})[38] and higher than for most recently reported ECP-based paper electrodes (Figure 4b). In addition, the corresponding volumetric power density was 3.5 W cm^{-3}, which likewise is comparable to the values for commercial carbon supercapacitors,[38] and, to the best of our knowledge, the highest reported value for a PPy-based electrode so far.[15,27,29,34,37] It should be pointed out that while commercial carbon based supercapacitors contain nonaqueous electrolytes which enable the attainment of higher cell voltages, the present ECP-based paper electrodes are used together with an aqueous electrolyte. Although the latter gives rise to a lower cell voltage the present data indicate that similar energy and power densities still can be obtained as a result of the higher inherent capacitance of the ECP electrodes.

The energy and power densities were also calculated with respect to the volume of the entire device (including separator and current collectors, cf. experimental section for details), to yield an energy density of 3.1 mWh cm^{-3} and a power density of 3 W cm^{-3}, while the latter energy density is similar to those of 4V-500μAh thin-film lithium batteries (0.3−10 mWh cm^{-3},[39] the present power density is about two orders or magnitude higher[39]). As is seen in Table S1 in the Supporting Information, the energy and power densities obtained in this work are generally high compared to the values for most of the ECP-based supercapacitors reported to date, particularly when considering the high mass loading of the present devices.

As is described in Figure 5, three symmetric supercapacitors were connected in series by stacking the PPy@c-NCFs electrode materials, separated by cellulose paper soaked with a 2 M NaCl solution, between graphite foil current collectors and sealing the device using plastic coated aluminum film (see the inset in Figure 5a). The flexibility of the resulting supercapacitor and the electrochemical performance of the device upon its bending were investigated. Upon bending the supercapacitors at a bending angle of ~340°, the charge/discharge profiles at ±20 mA maintained the triangular shape obtained for the flat, unbent state (see Figure 5b). The shape of the CV curves recorded at

a scan rate of 20 mV s^{-1} between 0 and 2.4 V were likewise essentially unchanged upon bending (see Figure S9) although the *iR*-drop was somewhat smaller for the bent supercapacitor. The latter was probably due to a lower contact resistance between the current collectors and the electrode materials induced by the applied pressure associated with the bending of the device.[40,41] Upon applying potential steps to 2.4 and 0 V, exponentially decaying current transients were observed both in the flat and in the bent state (see Figure 5c), indicating that the current was controlled by the RC time constant (*i.e.*, the cell capacitance and resistance) rather than the mass transport of counterions or the kinetics of the electrode reactions.[36] As is seen in Figure 5a and Video S1, the flexible supercapacitor was also able to power a light-emitting diode (LED) both in its flat and bent state (up to about 340°).

CONCLUSIONS

We demonstrate that densely packed polypyrrole-nanocellulose composites can be synthesized by chemical modification of pristine nanocellulose fibers without significant loss of flexibility, micro- and mesoporosity or ion-accessible surface area. Flexible and compact supercapacitors based on such composite paper electrodes can provide very high gravimetric and volumetric capacitances of 127 F g^{-1} and 122 F cm^{-3} based on the electrode mass/volume at current densities up to 300 mA cm^{-2} (or 33 A g^{-1}), as well as device-specific volumetric energy and power densities of 3.1 mWh cm^{-3} and 3 W cm^{-3}; values that to the best of our knowledge exceed those of other conducting polymer-based electric energy storage systems even though the latter values were obtained at significantly lower current densities and with significantly smaller mass loadings.

METHODS

Materials. The *Cladophora* nanocellulose was obtained from FMC Biopolymers. 2,2,6,6-Tetramethylpiperidine-1-oxyl radical (TEMPO), dimethyl sulfoxide (DMSO), hydrochloric acid, sodium hydroxide, glycidyltrimethylammonium chloride (EPTMAC), sodium bromide, sodium hypochlorite, isopropanol, hexamethyldisilazane (HMDS), glutaraldehyde, ethanol, iron(III) chloride hexahydrate, sodium chloride and pyrrole were all obtained from Sigma-Aldrich and used as received. Cellulose papers (Munktell, Sweden) were used as separators in the supercapacitors.

Preparation of Modified NCFs. Cationic (c-NCFs) and anionic (a-NCFs) modified *Cladophora* NCFs were synthesized as previously described.[28] For the a-NCFs, 10 g of *Cladophora* cellulose powder was dispersed in 1.4 L of deionized water ,and 0.52 g of NaBr and 0.05 g of TEMPO dissolved in 0.1 L of deionized water were added. The mixture was mixed with 0.1 L of 10% (w/w) NaClO. NaOH solution (0.5 M) was used to maintain pH 10.3 throughout the reaction. The reaction was quenched after 60 min by adding 20 mL of ethanol. The modified cellulose was washed and collected on a nylon filter. The as-obtained cellulose was redispersed in deionized water and ethanol and then spray-dried by a spray-dryer equipped with an inert loop (BUCHI Mini Spray Dryer B-290, Switzerland) with an outlet temperature of 95 °C and an inlet temperature of 180 °C. For the c-NCFs, a dispersion of 10 g of *Cladophora* cellulose in 20 mL of deionized water and 0.1 L of isopropanol was heated to 50 °C. An amount of 0.8 g of NaOH was added in 20 mL of deionized water, and 4.4 mL of EPTMAC was employed to initiate the reaction. The reaction was allowed to proceed for 2 h with stirring at 50 °C. The product was collected and thoroughly washed with deionized water and ethanol. The modified cellulose was resuspended and homogenized and subsequently spray-dried in a similar way as described for the a-NCFs.

Preparation of Compact PPy@NCFs Composites. Three different NCFs (0.1 g) were dispersed in 20 mL of water by sonication using a total pulse time of 10 min and water cooling. Volumes of 0.335 mL of pyrrole and 20 mL of 0.5 M HCl were mixed with the cellulose dispersion under stirring for 5 min. PPy was then formed on the NCFs by chemical polymerization employing oxidant solution (2.92 g of $FeCl_3 \cdot 6H_2O$ dissolved in 20 mL of 0.5 M HCl). The polymerization proceeded for 0.5 h under stirring after which the composite was collected on a Nylon membrane (0.45 μm) and washed with 2 L of 0.5 M HCl followed by 0.5 L of 0.1 M NaCl solution. The washed products were subsequently dried naturally to form paperlike sheets, yielding thicknesses of the as-obtained composite sheets of 130, 180, and 220 μm for PPy@c-NCFs, PPy@u-NCFs, and PPy@a-NCFs, respectively. The PPy weight ratio in the composites was about 70%, as determined from the weight of NCFs used in the preparation and the total composites weight after drying. All samples had a mass loading of ~13 mg cm^{-2}, which means that the areal active mass loading of PPy was ~9 mg cm^{-2}. The bulk density of a paper composite, that is, the ratio between the composite weight and volume, was estimated from the dimensions of a piece of paper composite, employing a high precision digital caliper (Mitutoyo, Japan). The densities of PPy@c-NCFs, PPy@u-NCFs, and PPy@a-NCFs were 0.96, 0.70, and 0.60 g cm^{-3}, respectively. The porosity of a sample was estimated as $\varepsilon_{\%} = (1 - \rho_b/\rho_t) \times 100$, where ρ_t and ρ_b denote the true density and bulk density, respectively. The porosities of the PPy@c-NCFs, PPy@u-NCFs, and PPy@a-NCFs were 38, 56, and 62%, respectively.

Fabrication of Symmetric Supercapacitors. Symmetric supercapcitors, hermetically heat-sealed in a coffee-bag arrangement, were assembled as previously described.[27] The PPy-NCF composites were directly used as electrodes without any conductive additives or additions of binders. Two pieces of the paper composites (~1.0 cm × 1.0 cm) were separated by a piece of ordinary filter paper, while Pt foils were used as the current collectors.

Structural Characterization and Analysis. SEM images for all samples were obtained using a Leo Gemini 1550 FEG SEM instrument (Zeiss, Germany). Nitrogen gas adsorption and desorption isotherms were recorded with an ASAP 2020 instrument (Micromeritics). The specific surface area was calculated according to the BET method during adsorption, and the pore size distribution was determined using the BJH method. Thermogravimetric analysis (TGA) was performed using a Mettler Toledo TGA/SDTA851 instrument. The composites were heated from 25 to 800 °C at a heating rate of 10 °C/min under air flow. Tensile strength measurements were performed using a Shimadzu Autograph AGS-X tensile machine. Rectangular strips (5 mm × 30 mm) were tested using a deformation rate of 0.001 mm S^{-1}. Fourier transform infrared (FTIR) spectroscopy measurements of the three types of NCF fibers employed were performed in attenuated total reflectance (ATR) mode with a Spectrum One FTIR spectrometer equipped with a Diamond/ZnSe crystal (PerkinElmer).

Electrochemical Characterization and Analysis. All electrochemical tests were performed with two-electrode symmetric supercapacitors at room temperature using an Autolab/GPES instrument (ECO Chemie, The Netherlands). The electrochemical impedance spectroscopy (EIS) measurements were collected at a cell potential of 0 V, using an ac amplitude of 10 mV employing

a frequency range between 100 kHz and 10 mHz. Galvanostatic charge−discharge measurements were done at different current densities between 1 and 300 mA cm^{-2} (a current density of 30 mA cm^{-2} was performed in the cycling stability tests) as the cell was charged to a voltage of 0.8 V.

The specific gravimetric electrode capacitance (C_g) was derived from the galvanostatic discharge curves using the formula: $C_g = 4I\Delta t/(m\Delta V)$, where I represents the discharge current, ΔV denotes the potential change during the discharge time Δt, while m refers the total weight of the two electrodes. The volumetric capacitance (C_v) was calculated by dividing the C_g value with the apparent density of the paper electrodes.

The volumetric energy density of the two electrodes ($E_{v\text{-electrode}}$) was normalized by the volume of both electrodes using the formulas $E_{v\text{-electrode}} = C_v(\Delta V)^2/8$. The procedure reported by Yang et al.[3] and Kaner et al.[42] was used to estimate the volumetric energy density of the entire device including two current collectors (each 12 μm thick), two electrodes, and the separator (20 μm thick). With this procedure, the volumetric device energy density is calculated by multiplying the volumetric energy density of two electrodes by the volumetric fraction of the two electrodes in the device. The volumetric power density normalized with respect to the volume of the electrodes ($P_{v\text{-electrode}}$) and device ($P_{v\text{-stack}}$) were calculated as

$$P_{v\text{-electrode}} = E_{v\text{-electrode}}/\Delta t, \quad P_{v\text{-stack}} = E_{v\text{-stack}}/\Delta t$$

Conflict of Interest: The authors declare no competing financial interest.

Acknowledgment. The Swedish Foundation for Strategic Research (SSF) (Grant RMA-110012), The Swedish Energy Agency (project SwedGrids), The Carl Trygger Foundation and The Bo Rydin Foundation are gratefully acknowledged for financial support of this work. ChangQing Ruan is acknowledged for assistance with the FTIR measurements.

Supporting Information Available: (Figure S1) FTIR measurements, (Figure S2) TGA curves, (Figure S3) tensile stress−strain curves, (Figure S4) N_2 adsorption/desorption isotherms, (Figure S5) charge/discharge curves recorded at different current densities, (Figure S6) cyclic voltammograms for nanocellulose and PPy@NCFs, (Figure S7) active mass normalized gravimetric and volumetric capacitances, (Figure S8) Ragone plots, and (Figure S9) cyclic voltammograms for the in-series supercapacitor device under flat and bent conditions; (Table S1) comparison of electrochemical performance of the flexible composite electrodes; (Video S1) video of the in-series supercapacitor device under flat and bent conditions. The Supporting Information is available free of charge on the ACS Publications website at DOI: 10.1021/acsnano.5b02846.

REFERENCES AND NOTES

1. Simon, P.; Gogotsi, Y.; Dunn, B. Where Do Batteries End and Supercapacitors Begin? *Science* **2014**, *343*, 1210–1211.
2. Ghidiu, M.; Lukatskaya, M. R.; Zhao, M. Q.; Gogotsi, Y.; Barsoum, M. W. Conductive Two-Dimensional Titanium Carbide "Clay" with High Volumetric Capacitance. *Nature* **2014**, *516*, 78–81.
3. Yang, X.; Cheng, C.; Wang, Y.; Qiu, L.; Li, D. Liquid-Mediated Dense Integration of Graphene Materials for Compact Capacitive Energy Storage. *Science* **2013**, *341*, 534–537.
4. Lukatskaya, M. R.; Mashtalir, O.; Ren, C. E.; Dall'Agnese, Y.; Rozier, P.; Taberna, P. L.; Naguib, M.; Simon, P.; Barsoum, M. W.; Gogotsi, Y. Cation Intercalation and High Volumetric Capacitance of Two-Dimensional Titanium Carbide. *Science* **2013**, *341*, 1502–1505.
5. Xu, Y.; Lin, Z.; Zhong, X.; Huang, X.; Weiss, N. O.; Huang, Y.; Duan, X. Holey Graphene Frameworks for Highly Efficient Capacitive Energy Storage. *Nat. Commun.* **2014**, *5*, 4554.
6. Kunowsky, M.; Garcia-Gomez, A.; Barranco, V.; Rojo, J. M.; Ibanez, J.; Carruthers, J. D.; Linares-Solano, A. Dense Carbon Monoliths for Supercapacitors with Outstanding Volumetric Capacitances. *Carbon* **2014**, *68*, 553–562.
7. Yan, J.; Wang, Q.; Wei, T.; Jiang, L.; Zhang, M.; Jing, X.; Fan, Z. Template-Assisted Low Temperature Synthesis of Functionalized Graphene for Ultrahigh Volumetric Performance Supercapacitors. *ACS Nano* **2014**, *8*, 4720–4729.
8. Yoon, Y.; Lee, K.; Kwon, S.; Seo, S.; Yoo, H.; Kim, S.; Shin, Y.; Park, Y.; Kim, D.; Choi, J.-Y.; Lee, H. Vertical Alignments of Graphene Sheets Spatially and Densely Piled for Fast Ion Diffusion in Compact Supercapacitors. *ACS Nano* **2014**, *8*, 4580–4590.
9. Jung, N.; Kwon, S.; Lee, D.; Yoon, D. M.; Park, Y. M.; Benayad, A.; Choi, J. Y.; Park, J. S. Synthesis of Chemically Bonded Graphene/Carbon Nanotube Composites and their Application in Large Volumetric Capacitance Supercapacitors. *Adv. Mater.* **2013**, *25*, 6854–6858.
10. Zhao, M. Q.; Ren, C. E.; Ling, Z.; Lukatskaya, M. R.; Zhang, C.; Van Aken, K. L.; Barsoum, M. W.; Gogotsi, Y. Flexible MXene/Carbon Nanotube Composite Paper with High Volumetric Capacitance. *Adv. Mater.* **2015**, *27*, 339–345.
11. Heon, M.; Lofland, S.; Applegate, J.; Nolte, R.; Cortes, E.; Hettinger, J. D.; Taberna, P.-L.; Simon, P.; Huang, P.; Brunet, M.; et al. Continuous Carbide-Derived Carbon Films with High Volumetric Capacitance. *Energy Environ. Sci.* **2011**, *4*, 135–138.
12. Chmiola, J.; Largeot, C.; Taberna, P.-L.; Simon, P.; Gogotsi, Y. Monolithic Carbide-Derived Carbon Films for Micro-Supercapacitors. *Science* **2010**, *328*, 480–483.
13. Snook, G. A.; Kao, P.; Best, A. S. Conducting-Polymer-Based Supercapacitor Devices and Electrodes. *J. Power Sources* **2011**, *196*, 1–12.
14. Nyholm, L.; Nyström, G.; Mihranyan, A.; Strømme, M. Toward Flexible Polymer and Paper-Based Energy Storage Devices. *Adv. Mater.* **2011**, *23*, 3751–3769.
15. Wang, Z.; Tammela, P.; Strømme, M.; Nyholm, L. Nanocellulose Coupled Flexible Polypyrrole@Graphene oxide Composite Paper Electrodes with High Volumetric Capacitance. *Nanoscale* **2015**, *7*, 3418–3423.
16. Yuan, L.; Yao, B.; Hu, B.; Huo, K.; Chen, W.; Zhou, J. Polypyrrole-Coated Paper for Flexible Solid-State Energy Storage. *Energy Environ. Sci.* **2013**, *6*, 470–476.
17. Xiong, G.; Meng, C.; Reifenberger, R. G.; Irazoqui, P. P.; Fisher, T. S. Graphitic Petal Electrodes for All-Solid-State Flexible Supercapacitors. *Adv. Energy Mater.* **2014**, *4*, 1300515.
18. Kim, M.; Lee, C.; Jang, J. Fabrication of Highly Flexible, Scalable, and High-Performance Supercapacitors Using Polyaniline/Reduced Graphene Oxide Film with Enhanced Electrical Conductivity and Crystallinity. *Adv. Funct. Mater.* **2014**, *24*, 2489–2499.
19. Meng, C.; Liu, C.; Chen, L.; Hu, C.; Fan, S. Highly Flexible and All-Solid-State Paperlike Polymer Supercapacitors. *Nano Lett.* **2010**, *10*, 4025–31.
20. Zhang, X.; Lin, Z.; Chen, B.; Zhang, W.; Sharma, S.; Gu, W.; Deng, Y. Solid-State Flexible Polyaniline/Silver Cellulose Nanofibrils Aerogel Supercapacitors. *J. Power Sources* **2014**, *246*, 283–289.
21. Meng, Y.; Wang, K.; Zhang, Y.; Wei, Z. Hierarchical Porous Graphene/Polyaniline Composite Film with Superior Rate Performance for Flexible Supercapacitors. *Adv. Mater.* **2013**, *25*, 6985–6990.
22. Yuan, L.; Xiao, X.; Ding, T.; Zhong, J.; Zhang, X.; Shen, Y.; Hu, B.; Huang, Y.; Zhou, J.; Wang, Z. L. Paper-Based Supercapacitors for Self-Powered Nanosystems. *Angew. Chem.* **2012**, *124*, 5018–5022.
23. Yao, B.; Yuan, L.; Xiao, X.; Zhang, J.; Qi, Y.; Zhou, J.; Zhou, J.; Hu, B.; Chen, W. Paper-Based Solid-State Supercapacitors with Pencil-Drawing Graphite/Polyaniline Networks Hybrid Electrodes. *Nano Energy* **2013**, *2*, 1071–1078.
24. Klemm, D.; Kramer, F.; Moritz, S.; Lindström, T.; Ankerfors, M.; Gray, D.; Dorris, A. Nanocelluloses: A New Family of Nature-Based Materials. *Angew. Chem., Int. Ed.* **2011**, *50*, 5438–5466.
25. Zheng, G.; Cui, Y.; Karabulut, E.; Wågberg, L.; Zhu, H.; Hu, L. Nanostructured Paper for Flexible Energy and Electronic Devices. *MRS Bull.* **2013**, *38*, 320–325.

26. Anothumakkool, B.; Soni, R.; Bhange, S. N.; Kurungot, S. Novel Scalable Synthesis of Highly Conducting and Robust PEDOT Paper for A High Performance Flexible Solid Supercapacitor. *Energy Environ. Sci.* **2015**, *8*, 1339–1347.
27. Wang, Z.; Tammela, P.; Zhang, P.; Strømme, M.; Nyholm, L. High Areal and Volumetric Capacity Sustainable All-Polymer Paper-Based Supercapacitors. *J. Mater. Chem. A* **2014**, *2*, 16761–16769.
28. Hua, K.; Carlsson, D. O.; Ålander, E.; Lindström, T.; Strømme, M.; Mihranyan, A.; Ferraz, N. Translational Study Between Structure and Biological Response of Nanocellulose From Wood and Green Algae. *RSC Adv.* **2014**, *4*, 2892–2903.
29. Wang, Z.; Tammela, P.; Zhang, P.; Huo, J.; Ericson, F.; Strømme, M.; Nyholm, L. Freestanding Nanocellulose-Composite Fibre Reinforced 3D Polypyrrole Electrodes for Energy Storage Applications. *Nanoscale* **2014**, *6*, 13068–13075.
30. Carlsson, D. O.; Mihranyan, A.; Strømme, M.; Nyholm, L. Tailoring Porosities and Electrochemical Properties of Composites Composed of Microfibrillated Cellulose and Polypyrrole. *RSC Adv.* **2014**, *4*, 8489–8497.
31. Carlsson, D. O.; Nyström, G.; Zhou, Q.; Berglund, L. A.; Nyholm, L.; Strømme, M. Electroactive Nanofibrillated Cellulose Aerogel Composites with Tunable Structural and Electrochemical Properties. *J. Mater. Chem.* **2012**, *22*, 19014–19024.
32. Wu, Q.; Xu, Y.; Yao, Z.; Liu, A.; Shi, G. Supercapacitors Based on Flexible Graphene/Polyaniline Nanofiber Composite Films. *ACS Nano* **2010**, *4*, 1963–1970.
33. Wang, D.-W.; Li, F.; Zhao, J.; Ren, W.; Chen, Z.-G.; Tan, J.; Wu, Z.-S.; Gentle, I.; Lu, G. Q.; Cheng, H.-M. Fabrication of Graphene/Polyaniline Composite Paper *via In Situ* Anodic Electropolymerization for High-Performance Flexible Electrode. *ACS Nano* **2009**, *3*, 1745–1752.
34. Razaq, A.; Nyholm, L.; Sjödin, M.; Strømme, M.; Mihranyan, A. Paper-Based Energy-Storage Devices Comprising Carbon Fiber-Reinforced Polypyrrole-Cladophora Nanocellulose Composite Electrodes. *Adv. Energy Mater.* **2012**, *2*, 445–454.
35. Wang, X.; Gao, K.; Shao, Z.; Peng, X.; Wu, X.; Wang, F. Layer-by-Layer Assembled Hybrid Multilayer Thin Film Electrodes Based on Transparent Cellulose Nanofibers Paper for Flexible Supercapacitors Applications. *J. Power Sources* **2014**, *249*, 148–155.
36. Nyström, G.; Strømme, M.; Sjödin, M.; Nyholm, L. Rapid Potential Step Charging of Paper-Based Polypyrrole Energy Storage Devices. *Electrochim. Acta* **2012**, *70*, 91–97.
37. Wang, Z.; Tammela, P.; Zhang, P.; Strømme, M.; Nyholm, L. Efficient High Active Mass Paper-Based Energy-Storage Devices Containing Free-Standing Additive-Less Polypyrrole-Nanocellulose Electrodes. *J. Mater. Chem. A* **2014**, *2*, 7711–7716.
38. Burke, A. R&D Considerations for the Performance and Application of Electrochemical Capacitors. *Electrochim. Acta* **2007**, *53*, 1083–1091.
39. Pech, D.; Brunet, M.; Durou, H.; Huang, P.; Mochalin, V.; Gogotsi, Y.; Taberna, P.-L.; Simon, P. Ultrahigh-Power Micrometre-Sized Supercapacitors Based on Onion-Like Carbon. *Nat. Nanotechnol.* **2010**, *5*, 651–654.
40. Tammela, P.; Wang, Z.; Frykstrand, S.; Zhang, P.; Sintorn, I.-M.; Nyholm, L.; Strømme, M. Asymmetric Supercapacitors Based on Carbon Nanofibre and Polypyrrole/Nanocellulose Composite Electrodes. *RSC Adv.* **2015**, *5*, 16405–16413.
41. Tammela, P.; Olsson, H.; Strømme, M.; Nyholm, L. The Influence of Electrode and Separator Thickness on the Cell Resistance of Symmetric Cellulose–Polypyrrole-Based Electric Energy Storage Devices. *J. Power Sources* **2014**, *272*, 468–475.
42. El-Kady, M. F.; Strong, V.; Dubin, S.; Kaner, R. B. Laser Scribing of High-Performance and Flexible Graphene-Based Electrochemical Capacitors. *Science* **2012**, *335*, 1326–1330.